PorphyStruct: A Digital Tool for the Quantitative Assignment of Non-Planar Distortion Modes in Four-Membered Porphyrinoids

Jens Krumsieck[a] and Martin Bröring*[a]

Dedicated to Mathias O. Senge on the occasion of his 60th anniversary

Abstract: *PorphyStruct*, a new digital tool for the analysis of non-planar distortion modes of different porphyrinoids, and its application to corrole structures is reported. The program makes use of the normal-coordinate structure decomposition technique (NSD) and employs sets of normal modes equivalent to those established for porphyrins in order to describe the *out-of-plane* dislocation pattern of perimeter atoms from corroles, norcorroles, porphycenes and other porphyrinoids quantitatively and in analogy to the established terminology. A comparative study of 17 porphyrin structures shows very similar results to the original NSD analysis and no systematic error. Application to corroles is successful and reveals the necessity to implement an extended basis of normal modes for a large share of experimental structures. The results frequently show the concomitant occurence of several modes but remain interpretable. For group XI metal corroles the phenomenon of supersaddling was unravelled, allowing for more in-depths discussions of structure-function correlations.

Introduction

Porphyrins, chlorins and related biomacrocycles are generally addressed as planar 18π aromatic systems, but the molecular structures almost always exhibit non-planar $C_{20}N_4$ perimeters.[1] The strength, nature and pattern of the deflection of perimeter atoms from a mean plane is determined by intermolecular effects such as crystal packing, supramolecular arrangements, or weak interactions within protein binding pockets on the one hand, and by intramolecular conditions such as metalation, axial ligation, and peripheral substitution on the other. Associated with the non-planar distortions[2] are changes in orbital energies, orbital symmetries and orbital mixtures. The fine-tuning of properties such as light absorption, excited state lifetimes, or stability of spin and oxidation states of bound metal ions is brought about by subtle non-planar conformational characteristics in many natural and non-natural porphyrinoid systems.[3]

Non-planar conformations can be assessed and quantitatively analysed for metal porphyrins and related systems with the same 24-membered perimeter using the technique of normal-coordinate structural decomposition (NSD) on crystallographically or theoretically determined molecular structures.[4] This technique has recently been modernised and made web-available by the Senge group.[5]

The NSD analysis separates the dislocations of the perimeter atoms from a mean plane according to the symmetries of the out-of-plane (*oop*) normal vibrations of a D_{4h} symmetric molecule into six different modes (Figure 1).[4,5] The three low-energy modes B_{2u}/saddling, B_{1u}/ruffling, and A_{2u}/doming are frequently discussed in the relevant literature, and their effects are well described in biomolecules as well as in model systems.[3m,6] In contrast, the remaining and higher-energy modes (E_g/waving and A_{1u}/propellering) occur only to an ancillary extent, and a unified interpretation of molecular or

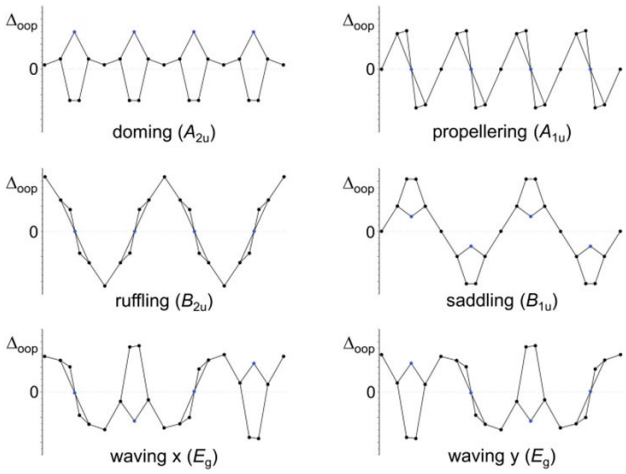

Figure 1. Linear display of metal porphyrin *oop* distortion modes.

[a] J. Krumsieck, Prof. Dr. M. Bröring
Institute for Inorganic and Analytical Chemistry
TU Braunschweig
Hagenring 30, 38102 Braunschweig (Germany)
E-mail: m.broering@tu-bs.de

Supporting information for this article is available on the WWW under https://doi.org/10.1002/chem.202101243

supramolecular parameters causing these distortions has to the best of our knowledge not yet been derived for metal porphyrins.[4a]

NSD analyses can also be successfully applied to non-metallated porphyrin ligands, even though, strictly speaking, a different minimal basis may have to be considered in these cases due to the lower symmetry (see below). The values obtained have nevertheless proven to be very helpful for the assessment and interpretation of molecular structures, so that the application of NSD may become a standard for the free bases, too. Analysing ring-modified porphyrinoids, especially isomeric, contracted and expanded porphyrinoids, however, is not possible in this way. For the structural interpretation of ring-contracted systems such as the naturally occurring corrins and the much-noted corroles, various geometric parameters have been discussed and used to describe related distortion modes.[7] However, these rather descriptive methods are unsuitable for a treatment of all modes and in particular do not give a hint for the contribution of a given distortion type.

We have now been looking for a method for the quantitative description of non-planar distortion modes comparable to the NSD analysis, which on the one hand retains the terminology of the NSD method, but on the other hand is flexible with respect to the size and shape of the macrocycle perimeter. In this paper, we describe our approach leading to the *PorphyStruct* program, compare our results for porphyrins with those from the original NSD analysis, and demonstrate the application upon corroles.

Results and Discussion

Porphyrinoid *out-of-plane* deformations in *PorphyStruct*

NSD and *PorphyStruct* describe the molecular structure of a porphyrin (solid state structure or calculated structure) by a linear combination of the normal modes as Equation (1):[4a]

$$D_{obs} = \sum_{\Gamma,\mathrm{m}} d_m^{\Gamma} D_m^{\Gamma} = \sum_{\Gamma} d_m^{\Gamma_{\mathrm{oop}}} D_m^{\Gamma_{\mathrm{oop}}} + \sum_{\Gamma} d_m^{\Gamma_{\mathrm{ip}}} D_m^{\Gamma_{\mathrm{ip}}} = D_{obs}^{oop} + D_{obs}^{ip} \quad (1)$$

For a metal porphyrin as a non-linear molecule, there are 3N-6 modes (or vibrational degrees of freedom), which results in 66 modes for the 24 framework atoms of the $C_{20}N_4$ perimeter. Of these, N-3 modes (21) are assigned to *out-of-plane* (*oop*) vibrations and 2N-3 modes (45) to *in-plane* (*ip*) vibrations. In the point group D_{4h}, there are five *oop* and *ip* symmetries each (B_{2u}, B_{1u}, A_{2u}, E_g(x,y), A_{1u}, and A_{1g}, A_{2g}, B_{1g}, B_{2g} and E_u(x,y), respectively), with one degenerate pair occurring in each case. The 21 *oop* modes to which the approach in this contribution is restricted are distributed among these symmetries as shown in Equation (2):[4a]

$$\Gamma_{oop} = 2\ A_{1u} + 3\ A_{2u} + 3\ B_{1u} + 3\ B_{2u} + 5\ E_g \quad (2)$$

Each symmetry can be assigned a specific conformation mode. Here A_{1u} stands for propellering, A_{2u} for doming, B_{1u} for saddling, B_{2u} for ruffling and E_g for waving x,y (Figure 1). The frequencies of the 21 modes can be determined by force field calculations from a structure chosen as a standard reference. Such reference should be as planar as possible in order to avoid admixture of the individual modes. If only the lowest energy mode within each symmetry is used for the analysis (the so-called minimal basis), almost all found metal porphyrin conformations can be described by this model with excellent accuracy. The *oop* modes are thereby represented as deflection pattern of the perimeter atoms from a mean plane, with the 24-membered perimeter of the porphyrins remaining as an invariable structural motif.

Three problems arise when attempting to transfer this approach to porphyrinoids with a varied framework. The first problem concerns the planar reference compounds. In the NSD, the crystallographically determined molecular structure of copper porphyrin **1** (Figure 2) is used for this purpose. *PorphyStruct* also uses this copper porphyrin as a reference, but as a DFT-optimised and perfectly D_{4h}-symmetric structure (B3LYP, def2-SVP with D3BJ dispersion). Contracted porphyrinoids such as the corroles or norcorroles, on the other hand, only rarely exist in a nearly planar form. Therefore, DFT structures of palladium(II) corrolate **2**[8] under enforcement of a C_{2v} symmetry, as well as of the nickel norcorrole **3**[9] under enforcement of a D_{2h} symmetry were used.[10] The enforcements are necessary to prevent a "contamination" of the normal modes by distortions occurring in the molecular minimum structures (cp. negative doming frequency of norcorrole, Table 1).

The second problem concerns the symmetry breaking that occurs upon the transition from the D_{4h}-symmetrical metal porphyrin to the C_{2v}-symmetrical metal corrole or to the D_{2h}-symmetrical metal norcorrole. For a metal corrole, for example, 20 *oop* normal modes are obtained, which are distributed over only two symmetries as shown in Equation (3):

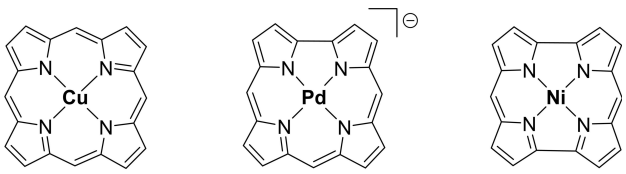

1 **2** **3**

Figure 2. Reference compounds for NSD and *PorphyStruct* normal modes.

Table 1. Frequencies/cm^{-1} and symmetries of metal porphyrin, corrole and norcorrole normal modes of the minimal basis.

	dom	sad	ruf	wav	pro
1 (D_{4h})	90 (A_{2u})	50 (B_{1u})	54 (B_{2u})	150 (E_g)	290 (A_{1u})
2 (C_{2v})	42 (B_1)	82 (A_2)	114 (B_1)	150 (B_1) 151 (A_2)	362 (A_2)
3 (D_{2h})	−26 (B_{3u})	89 (A_u)	140 (B_{3u})	96 (B_{1g}) 116 (B_{2g})	389 (A_u)

$$\Gamma_{oop} = 10\ A_2 + 10\ B_1 \quad (3)$$

The minimal basis for corroles thus consists only of A_2 (saddling) and B_1 (doming), which, however, is not sufficient for a description of real structures. Therefore, further modes were identified and assigned in analogy to the porphyrin case. In this fashion an equivalent set with doming (B_1), saddling (A_2), ruffling (B_1), waving x/y (B_1/A_2) and propellering (A_2) can be found within the normal modes, which allows a good description of many observed structures. In an analogous way, one can also obtain an acceptable minimal basis for other perimeter shapes. Table 1 lists the symmetries and the frequencies of the minimal basis modes shown in Figure 3 for metal porphyrins, metal corroles and metal norcorroles.[11]

While the absolute value of the vibrational frequencies for the individual modes in Table 1 is considered insignificant,[4a] the energetic order is realistic. For porphyrin, the orders used in *PorphyStruct* and NSD are identical. However, the order is different for different macrocycles. In particular, for both ring-contracted species shown in Table 1, the doming mode is the lowest in energy, while the ruffling mode is significantly raised. The peculiar negative doming frequency for metal norcorrole corresponds to a non-planar minimum structure of this compound, which has in fact been observed in calculated structures before.[12]

The supposed biggest hurdle in applying NSD to ring-variant porphyrinoids is the perimeter determination and fitting algorithm. For the *PorphyStruct* tool, this algorithm has been split up into two parts. In the first part, the macrocycle is recognised from the atomic coordinates by a graph theoretical approach and the appropriate reference structure, which is stored in the software, is selected on the basis of the recognised perimeter. In the second step, the deflections of the perimeter atoms from a mean plane are used to determine D_{oop}, analogous to the procedure in the NSD. *PorphyStruct* also uses this procedure for the reference structures to set up a reference matrix A_{ref} with the Euclidean normalised Y-axes and solves the following system of equations for the vector X (the result of the individual modes in Å) using the algorithm for matrix QR decomposition[13] with Equation (4):

$$A_{ref}{}^{*}X = D_{obs} \quad (4)$$

PorphyStruct uses any .xyz, .cif, and .mol2 files as input formats, and simply loads these by drag-and-drop. When analysing crystallographic structures, disorder and co-crystallisates are automatically removed or neglected. If there is more than one molecular structure in the asymmetric unit, all individually different molecules are recognised and analysed separately, producing colour coded results to choose from (see Supporting Information). The graphical and numerical output of *PorphyStruct* is similar to the one of the NSD web-tool,[5] but the analysis is limited to the occurrence and quantification of the *oop* normal modes. Several file formats can be chosen for output and storage of data and diagrams. In addition, frequently used and helpful structural parameters like the above mentioned dihedral angles, helicity, interplanar angle etc. are automatically produced (Figure 4). A comparison of the best fit of the theory with the molecular structure is also

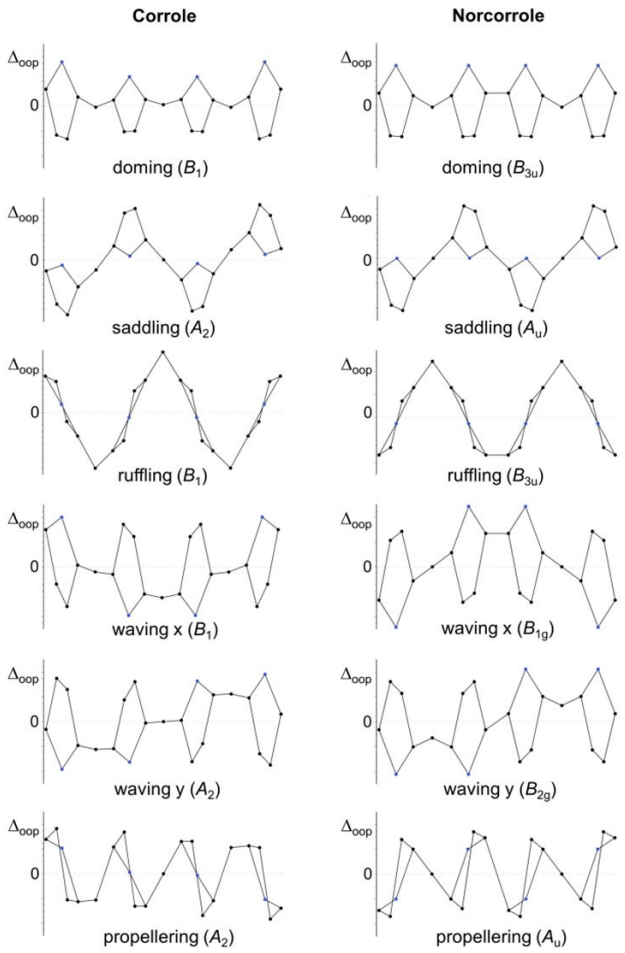

Figure 3. Linear display representations of metal corrole and norcorrole minimal basis normal modes.

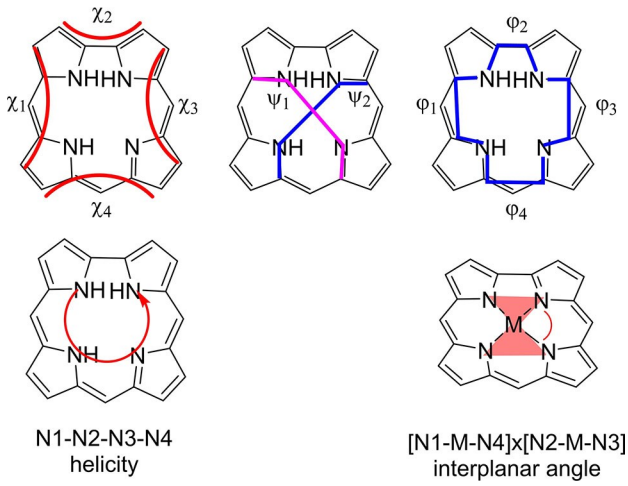

Figure 4. Definitions of helicity and special angles on the corrole framework, as given by the *PorphyStruct* output.

provided and allows for simple assessment of the quality and plausibility of the analyses.

PorphyStruct and NSD analyses of porphyrin structures

As a proof of concept, seventeen porphyrin structures were examined with *PorphyStruct* and the results were compared with those of the NSD analysis[4a] (Table 2). In order to enable a comprehensive comparison, the absolute values for the total distortion D_{oop} and the deviation from the NSD results for the different *oop* conformational modes were calculated. For this purpose, the contribution of the major mode to the total distortion is listed. In addition, the differences between the *PorphyStruct* and the NSD results are given for each mode.

As Table 2 shows, the *PorphyStruct* values for the total distortion D_{oop} are at or very close to the values from the NSD analysis in all examined cases. The differences, if any, are small and rarely exceed 1% of the absolute value. The largest difference is found for nickel-porphyrin **6** with slightly above 1%. Significant differences between the results of the two methods are uncovered neither for particularly large nor for particularly small D_{oop} values, and the presence and extent of certain distortion modes has not led to a particular preference. The same applies to different metal ions as well as to the free bases.

The mean value of the saddling mode is weighted lower by *PorphyStruct* than by the NSD analysis (maximum value −1.7% for **13**). The ruffling mode, on the other hand, is slightly accentuated in *PorphyStruct*. The average doming mode contribution remains the same by both methods, and the propellering mode plays only a very minor role throughout. Overall, there are no significant specific differences between the results of the two analysis methods. In particular, very similar distributions of the *oop* modes are obtained within a given total distortion. For the selected set of molecular structures, the minor deviations certainly do not stem from a different treatment due to the nature of the compounds, but probably from the use of slightly different references for the overall structural assessment.

Corroles

Beside the natural corrins, corroles are arguably the ring-contracted porphyrinoids which draw the most scientific attention. This macrocycle has occasionally been discussed in the past with respect to non-planar distortion modes and the influence of those on electronic structures and reactivities.[7b,d,l;31] We have therefore chosen this tetrapyrrole and discuss here some specific findings we unravelled using *PorphyStruct* analyses on experimental structures obtained through the Cambridge Crystallographic Data Centre (CCDC).

Non-planarity of free corrole bases

In the N_4 cavity of experimental structures of non-metallated porphyrins, there are two protons typically in a *trans* position with respect to each other. The mutual repulsion of these protons generally leads to a B_{2g} symmetric *in-plane* distortion,[5] so that most free base porphyrins do not deviate significantly from a planar structure unless they are forced by a sterically active periphery. Therefore a weak saddling distortion is the most frequently observed *oop* mode for the free bases.

The conditions are different for the free corrole bases. The presence of a third proton inside of the N_4 cavity of the corrole leads to stronger repulsion of the NH groups and thus to the rotation of the C_4N rings out of a mean macrocycle plane. An almost planar structure is only found for the corrole radical,[7c]

Table 2. Comparison of *PorphyStruct* and NSD results on 17 porphyrin structures.

	Compound[a]	D_{oop} (ΔD_{oop})[b]	Major mode [%]	Δ_{dom} [%]	Δ_{sad} [%]	Δ_{ruf} [%]	Δ_{wav} [%][c]	Δ_{pro} [%]
4	(tpp)Fe(py)$_2$[14]	0.828 (+/−0)	ruf 54.97	−0.19	−1.39	+1.19	+0.34	+0.05
5	(tpp)Co(H$_2$O)Cl[15]	1.546 (+/−0)	ruf 61.34	−0.13	−1.45	+1.48	+0.10	+/−0
6	(p)Ni[16]	0.088 (−0.001)	ruf 56.52	−0.17	+0.04	−1.87	+2.33	−0.33
7	(oep)Ni A[17]	0.079 (+/−0)	wav 99.93	+/−0	+0.01	+0.04	−0.07	+0.01
8	(oep)Ni B[18]	0.136 (+/−0)	wav 99.95	+/−0	+0.01	+0.03	−0.05	+0.01
9	(oep)Ni C[19]	1.461 (+/−0)	ruf 93.15	+/−0	−0.54	+0.47	+0.07	+/−0
10	(tmp)Ni[20]	0.314 (+/−0)	wav 55.94	+0.07	−0.71	−0.06	+0.92	−0.22
11	(oetpp)Ni[21]	3.817 (+/−0)	sad 93.87	+0.05	−0.32	+0.01	+0.26	+/−0
12	(dtBup)Ni[22]	2.243 (−0.006)	ruf 77.00	−0.54	+0.02	+0.58	−0.03	−0.02
13	(dptetmp)Ni[23]	1.220 (+0.001)	sad 76.76	+0.02	−1.71	+0.09	+1.48	+0.12
14	(tpp)Cu[24]	1.204 (+/−0)	ruf 87.64	+0.01	−1.11	+1.04	+0.07	+0.01
15	(hetmp)Cu[25]	1.741 (+/−0)	ruf 72.67	−0.30	−0.45	+0.86	−0.05	−0.05
16	(tnpcp)Zn(py)[26]	0.710 (+/−0)	dom 67.60	−0.18	+/−0	−0.15	−0.03	+0.06
17	(tpp)Tl(CN)[27]	0.497 (+/−0)	dom 63.99	+1.25	−0.11	+0.48	−1.69	+0.06
18	H$_2$(p)[28]	0.104 (+/−0)	ruf 56.61	−0.92	−0.05	−1.67	+2.59	−0.05
19	H$_2$(oep)[29]	0.126 (+/−0)	wav 99.86	+0.03	+0.03	+0.05	−0.14	+0.03
20	H$_2$(dppf28)[30]	0.660 (+/−0)	wav 99.99	+0.01	+/−0	+/−0	−0.01	+/−0

[a] tpp = dianion of 5,10,15,20-tetraphenylporphyrin; p = dianion of porphyrin; oep = dianion of 2,3,7,8,12,13,17,18-octaethylporphyrin; tmp = dianion of 5,10,15,20-tetramethylporphyrin; oetpp = dianion of 2,3,7,8,12,13,17,18-octaethyl-5,10,15,20-tetraphenylporphyrin; dtBup = dianion of 5,15-di-*t*-butylporphyrin; dptetmp = dianion of 5,15-diphenyl-2,8,12,18-tetraethyl-3,7,13,17-tetramethylporphyrin; hetmp = dianion of 2,5,8,12,15,18-hexaethyl-3,7,13,17-tetramethylporphyrin; tnpcp = dianion of tetra-(nitrophenyl)chiroporphyrin; dpp-f28 = dianion of 2,3,7,8,12,13,17,18-octa-4-fluorophenyl-5,10,15,20-tetrakis (pentafluorophenyl)porphyrin. [b] $\Delta D_{oop} = D_{oop}$(*PorphyStruct*) − D_{oop}(NSD). [c] The waving value wav is determined to wav = |wav x| + |wav y|.

as only two inner protons are present here, which minimises the repulsion. Moreover, for the evaluation of corrole structures, not only different conformations have to be taken into consideration, but basically also two different tautomeric forms, which are characterised by the binding of one or two protons to the bipyrrole subunit (Figure 5). In most known cases, oligopyrrolic macrocycles containing bipyrroles carry two protons on this substructure,[32] and in the case of corrole, calculations and measurements prove that the most stable tautomer is form **I** with two bipyrrolic protons (Figure 5).[33] For the sake of simplicity, the following analysis is limited to this preferred tautomer.

From simple geometrical considerations, two of the six *oop* modes can be expected to be energetically favourable for free corrole bases. On the one hand, it appears attractive if the three neighbouring C_4NH rings of the corrole core are alternately rotated upwards and downwards from a mean plane. This is equivalent to a saddling conformation, although there should still be residual repulsive forces between the two opposing protons. As an alternative, a *cis* instead of *trans* repulsion can be considered, especially for structures that are not too distorted. This is equivalent to a waving x mode in which both bipyrrolic NH groups are dislocated to the same side of the macrocycle mean plane, and the opposite N-H·N unit to the other. The alternatively conceivable waving y conformation, however, is less favourable, since here a *cis* repulsion occurs within a dipyrromethene unit, which appears energetically raised due to the NH functions pointing stronger towards each other (Figure 5).

For a *PorphyStruct* analysis, 69 structures of *meso*-substituted free corrole bases were obtained from the CCDC database (see Supporting Information) and the results of the structure simulations were first evaluated with regard to their validity. In all cases where the theoretical total distortion D_{oop}(sim) deviated from the experimental values by more than 3%, the minimal basis was considered to be an unsuitable standard and the results were not used any further. Of the 52 structures remaining, 38 showed an average distortion value D_{oop}(exp) between 0.6 and 1.0. Stronger distortions up to D_{oop}(exp) = 1.8 were obtained from 14 structures (Figure 6). The distribution of the individual *oop* modes among the structures with mean values of total distortion results in the expected dominance of

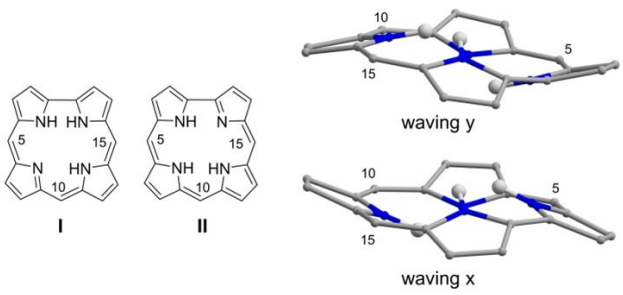

Figure 5. Tautomeric forms of corrole **I** and **II**, and representation of hydrogen atom locations within the waving x and waving y distortions of form **I**.

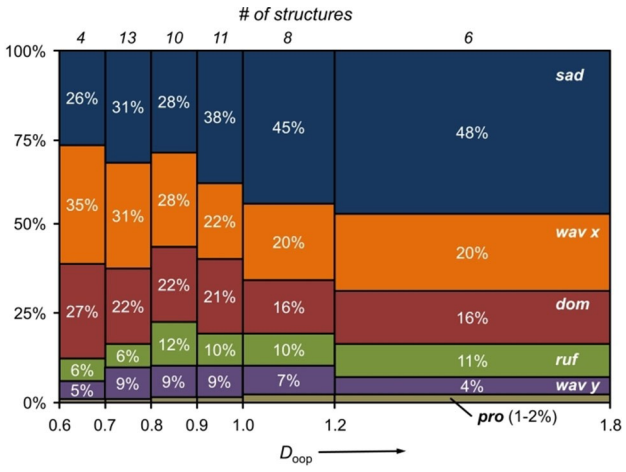

Figure 6. *Out-of-plane* distortion mode distribution of experimental free base corrole structures. Compounds are grouped for the extent of total distortion D_{oop}.

saddling (36%) and waving x (26%), and also assigns the doming mode a still significant 20% share of the total distortion. Waving y, ruffling and propellering, on the other hand, are significantly less involved with only 8%, 9% and 1%, respectively. With increasing total *oop* distortion, the importance of the saddling mode increases markedly until it reaches a value of 58% for the most distorted molecule at $_{oop}$(exp) = 1.8. Here, all corroles with sterically encumbered periphery are found at high D_{oop} values. As in the case of the corresponding porphyrins, a high degree of substitution thus also particularly strengthens the saddling mode of the corroles. The relatively strong waving x mode in undisturbed free corrole bases shows the stronger repulsion of *trans*-NH groups in this ring-contracted porphyrinoid, which appears feasible with respect to the smaller N_4 cavity size.

Metal corrole conformations

For the investigation of metal corrole structures, 114 data sets from the Cambridge Crystallographic Data Centre (CCDC; see Supporting Information) were analyzed with *PorphyStruct* with respect to *oop* distortions. In 49 cases, models were obtained for which the deviation from the experimental structure was larger than 3%. Apparently, for many metal corroles the use of the minimal basis from the 6 metal porphyrin-analogous modes of lowest energy is not sufficient for a comprehensive description of their non-planarity. For this reason, and similar to a routine used within the NSD analysis, an extended basis was generated, which additionally contains the energetically second lowest modes of the 6 respective distortions (Figure 7). With this extended basis, 113 of the 114 structures could be described satisfactorily. The remaining structure, which still has an error of >7% even with the parameters of the extended basis, was not considered further.

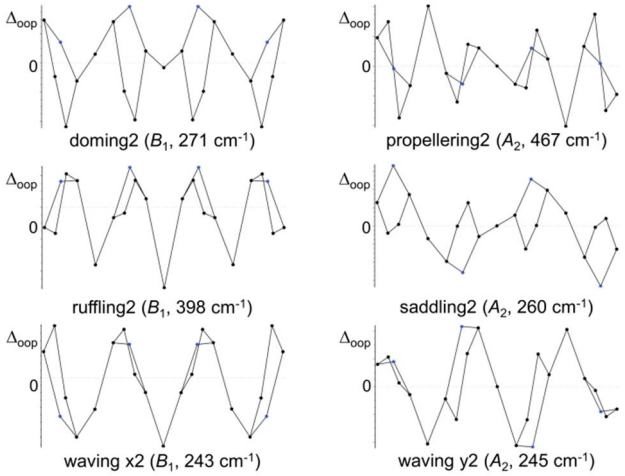

Figure 7. Second set of metal corrole distortion modes with symmetries and frequencies, used for the extended basis.

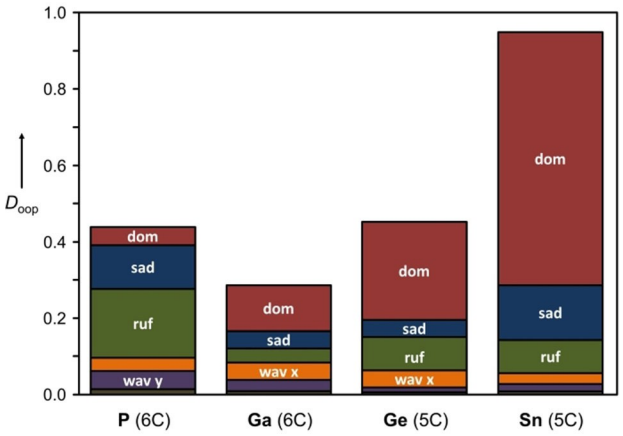

Figure 8. *Out-of-plane* distortion mode distribution and total distortion D_{oop} of selected main group metal corrole structures.

The results of the *PorphyStruct* analysis clearly demonstrate that the observable non-planar modes of metal corroles, as in the case of metal porphyrins, occur as a result from different intra- and intermolecular conditions. The modes are strongly dependent on the metal ions (ion radius and electronic configuration as well as coordination number) and the axial ligands (number, and steric demand by size and shape). As for the free corrole bases, this is overlaid by the substitution pattern of the tetrapyrrole. For similar compounds different major modes are sometimes found, indicating the supramolecular influence of crystal packing motifs. For a more detailed description, a treatment of metal corroles in selected groups is therefore advantageous.

Main group corroles. Of the 20 structures containing five- and six-coordinate (5C and 6C) main group central atoms from the groups XIII (Al, Ga), XIV (Ge, Sn) and XV (P, Sb), 13 could be described satisfactorily with the minimal basis. For the sake of comparability, all structures were thus analysed with the extended basis (see Supporting Information). Figure 8 shows averaged results for typical subgroups with large and small central atoms in different coordination numbers.

The result of the analysis shows that in most cases all modes except for propellering are present to a significant extent. The waving modes of the main group corroles appear to be stronger for the 6C species. Pronounced doming modes are shown by the 5C compounds of Ge and Sn. In the generally less distorted 6C structures, however, these modes also occur in intermediate total values, and can even be the major modes as for Ga. Saddling modes, on the other hand, are rather underrepresented. The presence of ruffling modes shows some dispersion among the compounds of this selected subgroup, with the small 6C phosphorus(V) derivatives providing the most ruffled macrocycles. Thus, a dependency on the ion size and the coordination number on the non-planar distortion pattern is clearly discernible, although the number of available experimental structures is still too small for a strong statement to be made.

Chromyl corroles. Besides the phosphorus(V) corroles, ruffling modes have also been reported in the literature for chromyl corroles with the small Cr(V) central atom.[7i] A *PorphyStruct* analysis of 7 structures (6 x *meso*-triaryl, 1x β-octaalkyl substitution) with the minimal basis succeeds only in two cases, so that the extended basis is used again. The compounds reveal a D_{oop} value for the overall distortion of 0.39–0.68, and significant doming modes of 0.19–0.44 Å, with the octaalkyl compound being the most distorted species. With two exceptions, the saddling modes are only slightly pronounced, but the described ruffling modes are indeed also found in this analysis throughout all compounds with values between 0.19 Å and 0.51 Å. On average, a picture emerges for the chromyl corroles in which 30.0% of the total distortion can be attributed to doming and 31.7% to ruffling. Nevertheless, the saddling modes with 21.9% and the waving modes with a combined 14.8% are also significantly involved in the *out-of-plane* conformation. The *PorphyStruct* analysis thus allows a much more differentiated picture of the existing structures then earlier geometric descriptions could do, mainly through the quantification of individual mode contributions.

(5C)-Mn(IV) corroles. 8 examples of pentacoordinated manganese(IV) corroles with axial halogen or aryl substitution were analysed (see Supporting Information). In all cases, the minimal basis proves to be sufficient. Surprisingly, the structures are very different from each other and a comparison in terms of a preferred conformation does not reveal any clear molecular correlation. Thus, depending on the case, doming, saddling or ruffling appears as the main distortion mode, and a second mode is usually enhanced, too. Apparently, intermolecular interactions are of particular importance in this group. The strong doming of the chlorido derivatives, the lesser overall distortion of the Mn(aryl) derivatives **21** and **22**,[34] and the strong differentiation of the waving modes are striking (Figure 9), although possibly not relevant within a larger picture due to the small number of comparative data sets. For an interpretation of these findings, more structural data will be necessary in the future.

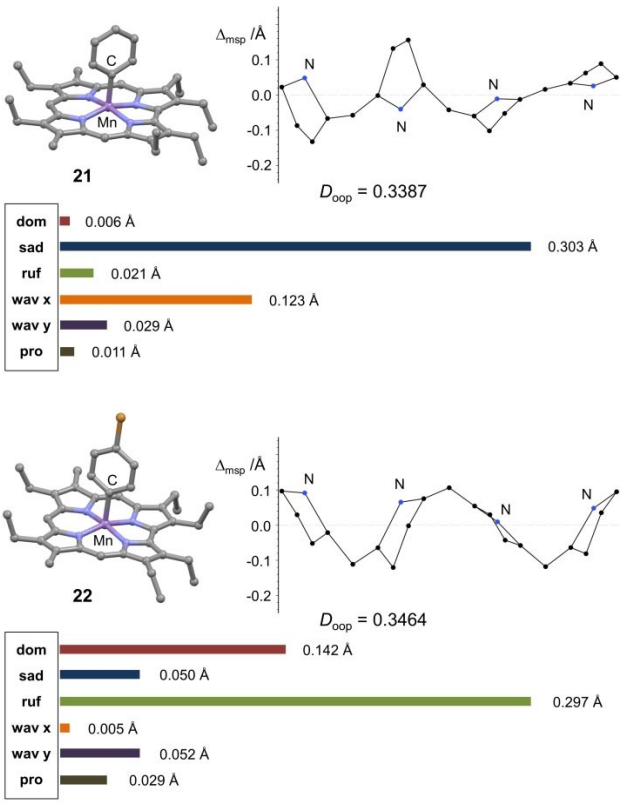

Figure 9. *PorphyStruct* results for two Mn(aryl)corroles **21** and **22**, using the minimal basis. Top rows: molecular structure and linear display of non-planar distortions. Bottom rows: colour-coded bar plots of the contributions of the six lowest-energy porphyrin-like normal modes to the overall distortion D_{oop}.

Coinage Metal Corroles. The most prominent group of metal corroles with specific non-planar distortion pattern recognised so far is the copper corroles. A concise saddling conformation is documented in the literature. This conformation is associated with the occurrence of a non-innocent corrole radical dianion ligand in these compounds and an antiferromagnetic interaction of the Cu 3d(x^2-y^2) electron with the corrole π radical. Thirteen structures of copper, silver and gold corroles could be analysed with *PorphyStruct*, and in all but one Au case the use of the extended basis is advised (see Supporting Information). In fact, for this group of compounds the minimal basis yields by far the largest deviations of up to 67.1 % from the experimental structures. The literature-known dominance of the saddling mode could indeed be proven in all cases. Figure 10 illustrates a typical result.[7b]

In fact, the Cu and Ag corroles are the only substances investigated so far to always reveal a very distinctive saddling2 mode, and frequently an enhanced waving y (with 10- and 11-fold substitution of the corrole) or waving y2 mode. Cu and Ag corroles can therefore be considered to display a supersaddling conformation. Such supersaddling is also found in one of the two Au corrole cases studied. The other modes are - with a few exceptions - only very weak.

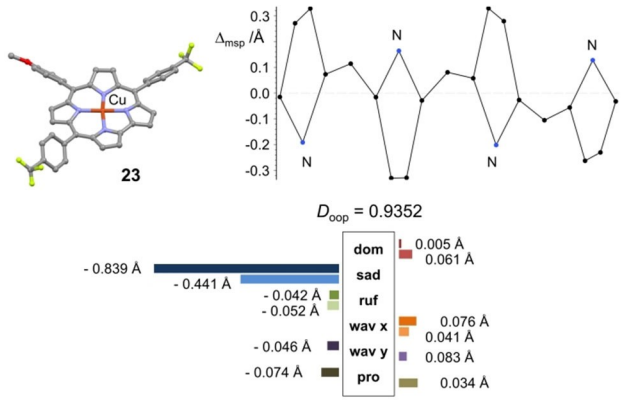

Figure 10. Supersaddling of a typical copper corrole **23**:[7b] *PorphyStruct* analysis result, using the extended basis. Top row: molecular structure and linear display of non-planar distortions. Bottom row: colour-coded bar plot of the contribution of the lowest-energy (dark) and second-lowest-energy porphyrin-like normal modes (bright) to the overall distortion D_{oop}.

Conclusion

PorphyStruct is now available for analysing non-planar distortion modes of many porphyrinoids like corroles, corrphycenes, porphycenes, heterocorroles, isocorroles, corrolazines and norcorroles, all of which show great potential for a functional analysis of their molecular structures. We could show that the non-planar conformations of porphyrinoids with perimeters deviating from the porphyrin one can be satisfactorily described by a set of normal modes. The selection of these modes is achieved by comparing the deflection diagrams with the known *oop* modes of metal porphyrins, whereby the use of an analogous set of six modes as a minimal basis is sufficient in many cases. An extended basis, which additionally contains the second lowest-energy mode of each type, can also been established for the treatment of structures that cannot be satisfactorily described with the minimal basis.

The usability of the new tool was proven by applying it to experimental structures of corroles and metal corroles. Here it is shown that the reduced symmetry of the porphyrinoids often leads to the occurrence of more than one major individual mode for the description of a given non-planarity pattern. In many cases, doming, saddling and ruffling modes are found side by side, and waving x/y modes are also more prominent than within porphyrin structures. An interpretation of the results along the lines known for the porphyrins is nevertheless possible. For example, the interpretation of a ruffling mode as an adaptation of the macrocycle perimeter to a very small central atom still applies to corroles, but is not an exclusive explanation. Similarly, saddling is also motivated in corroles by large central atoms and an overloaded periphery, although waving modes are increasingly interfering. A special feature associated with the use of the extended basis is the phenomenon of supersaddling, in which the saddling2 mode comes to the side of the saddling mode to a significant extent. The interpretation of such findings will become more straightfor-

ward as more structures will become available and analysed in the future.

Implementation and Availability

PorphyStruct was written in the object-oriented programming language C# based on .NET 5.0. For the calculation of the mean plane and the composition of the normal modes, the matrix SVD and matrix QR algorithms from the MathNET.Numerics[13] program package were used. The processing of the files (cif, xyz, mol2) is done by means of code which was stored in a separate library[35] for reasons of reusability. The linear display diagrams were realised using the cross-platform plotting library OxyPlot,[36] the 3D molecular structures using Helix Toolkit.[37] For the user interface and implementation of the MVVM software design pattern, further open-source libraries were used.[38]

The source code of *PorphyStruct* is available/viewable at https://github.com/JensKrumsieck/PorphyStruct. The software can be downloaded at https://github.com/JensKrumsieck/PorphyStruct/releases/latest.

Acknowledgements

Open access funding enabled and organized by Projekt DEAL.

Conflict of Interest

The authors declare no conflict of interest.

Keywords: conformation · corrole · digital tools · molecular structure · porphyrin

[1] a) E. B. Fleischer, *J. Am. Chem. Soc.* **1963**, *85*, 146–148; b) E. B. Fleischer, *J. Am. Chem. Soc.* **1963**, *85*, 1353–1354; c) A. Stone, E. B. Fleischer, *J. Am. Chem. Soc.* **1968**, *90*, 2735–2748; d) E. B. Fleischer, *Acc. Chem. Res.* **1970**, *3*, 105–112; e) C. Kratky, R. Waditschatka, C. Angst, J. E. Johansen, J. C. Plaquevent, J. Schreiber, A. Eschenmoser, *Helv. Chim. Acta* **1985**, *68*, 1312–1316.

[2] J. Takeda, T. Ohya, M. Sato, *Inorg. Chem.* **1992**, *31*, 2877–2880.

[3] a) K. M. Barkigia, L. Chantranupong, K. M. Smith, J. Fajer, *J. Am. Chem. Soc.* **1988**, *110*, 7566–7567; b) E. Gudowska-Nowak, M. D. Newton, J. Fajer, *J. Phys. Chem.* **1990**, *94*, 5795–5801; c) C. J. Medforth, J. J. Smith, *Tetrahedron Lett.* **1990**, *31*, 5583–5586; d) J. A. Shelnutt, C. J. Medforth, M. D. Berber, K. M. Barkigia, K. M. Smith, *J. Am. Chem. Soc.* **1991**, *113*, 4077–4087; e) K. M. Kadish, E. van Caemelbecke, P. Boulas, F. D'Souza, E. Vogel, M. Kisters, C. J. Medforth, K. M. Smith, *Inorg. Chem.* **1993**, *32*, 4177–4178; f) W. Jentzen, M. C. Simpson, J. D. Hobbs, X. Song, T. Ema, N. Y. Nelson, C. J. Medforth, K. M. Smith, M. Veyrat, M. Mazzanti, R. Ramasseul, J. C. Marchon, T. Takeuchi, W. A. Goddard, J. A. Shelnutt, *J. Am. Chem. Soc.* **1995**, *117*, 11085–11097; g) W. W. Kalisch, M. O. Senge, *Tetrahedron Lett.* **1996**, *37*, 1183–1186; h) M. O. Senge, W. W. Kalisch, *Inorg. Chem.* **1997**, *36*, 6103–6116; i) M. O. Senge, M. W. Renner, W. W. Kalisch, J. Fajer, *J. Chem. Soc. Dalton Trans.* **2000**, 381–385; j) R. E. Haddad, S. Gazeau, J. Pécaut, J.-C. Marchon, C. J. Medforth, J. A. Shelnutt, *J. Am. Chem. Soc.* **2003**, *125*, 1253–1268; k) M. O. Senge, *Chem. Commun.* **2006**, 243–256; l) M. Senge, A. Ryan, K. Letchford, S. MacGowan, T. Mielke, *Symmetry* **2014**, *6*, 781–843; m) M. O. Senge, S. A. MacGowan, J. M. O'Brien, *Chem. Commun.* **2015**, *51*, 17031–17063.

[4] a) W. Jentzen, X.-Z. Song, J. A. Shelnutt, *J. Phys. Chem. B* **1997**, *101*, 1684–1699; b) W. Jentzen, J.-G. Ma, J. A. Shelnutt, *Biophys. J.* **1998**, *74*, 753–763.

[5] C. J. Kingsbury, M. O. Senge, *Coord. Chem. Rev.* **2020**, *431*, 213760. For web access, see https://www.sengegroup.eu/nsd.

[6] a) Z. Zhou, M. Shen, C. Cao, Q. Liu, Z. Yan, *Chem. Eur. J.* **2012**, *18*, 7675–7679.

[7] a) S. Ye, T. Tuttle, E. Bill, L. Simkhovich, Z. Gross, W. Thiel, F. Neese, *Chem. Eur. J.* **2008**, *14*, 10839–10851; b) A. B. Alemayehu, E. Gonzalez, L. K. Hansen, A. Ghosh, *Inorg. Chem.* **2009**, *48*, 7794–7799; c) P. Schweyen, K. Brandhorst, R. Wicht, B. Wolfram, M. Bröring, *Angew. Chem. Int. Ed.* **2015**, *54*, 8213–8216; *Angew. Chem.* **2015**, *127*, 8331–8334; d) J. Rösner, B. Cordes, S. Bahnmüller, G. Homolya, D. Sakow, P. Schweyen, R. Wicht, M. Bröring, *Angew. Chem. Int. Ed.* **2017**, *56*, 9967–9970; *Angew. Chem.* **2017**, *129*, 10099–10102; e) M. M. Kruk, D. V. Klenitsky, W. Maes, *Macroheterocycles* **2019**, *12*, 58–67; f) C. Klieninger, E. Deery, A. D. Lawrence, M. Podewitz, K. Wurst, E. Nemoto-Smith, F. J. Widner, J. A. Baker, S. Jockusch, C. R. Kreutz, K. R. Liedl, K. Gruber, M. J. Warren, B. Kräutler, *Angew. Chem. Int. Ed.* **2019**, *58*, 10756–10760; *Angew. Chem.* **2019**, *131*, 10869–10873; g) C. Klieninger, J. A. Baker, M. Podewitz, K. Wurst, S. Jockusch, A. D. Lawrence, E. Deery, K. Gruber, K. R. Liedl, M. J. Warren, B. Kräutler, *Angew. Chem. Int. Ed.* **2019**, *58*, 14568–14572; *Angew. Chem.* **2019**, *131*, 14710–14714; h) M. M. Kruk, D. V. Klenitsky, L. L. Gladkov, W. Maes, *J. Porphyrins Phthalocyanines* **2020**, *24*, 765–774; i) P. Schweyen, C. Kleeberg, D. Körner, A. Thüsing, R. Wicht, M.-K. Zaretzke, M. Bröring, *J. Porphyrins Phthalocyanines* **2020**, *24*, 303–313; j) C. Klieninger, K. Wurst, M. Podewitz, M. Stanley, E. Deery, A. D. Lawrence, K. R. Liedl, M. J. Warren, B. Kräutler, *Angew. Chem. Int. Ed.* **2020**, *59*, 20129–20136; *Angew. Chem.* **2020**, *132*, 20304–20311; k) Q. Liu, J. Zhang, M. Tang, Y. Yang, J. Zhang, Z. Zhou, *Org. Biomol. Chem.* **2018**, *16*, 7725–7736.

[8] Q.-C. Chen, N. Fridman, Y. Diskin-Posner, Z. Gross, *Chem. Eur. J.* **2020**, *26*, 9481–9485.

[9] T. Ito, Y. Hayashi, S. Shimizu, J.-Y. Shin, N. Kobayashi, H. Shinokubo, *Angew. Chem. Int. Ed.* **2012**, *51*, 8542–8545; *Angew. Chem.* **2012**, *124*, 8670–8673.

[10] The porphyrin isomers porphycene and corrphycene are also implemented in *PorphyStruct*, using the DFT structures of the zinc(II) derivatives as references.

[11] *Chemcraft - Graphical software for visualization of quantum chemistry computations*, https://www.chemcraftprog.com.

[12] a) J. Conradie, C. Foroutan-Nejad, A. Ghosh, *Sci. Rep.* **2019**, *9*, 4852; b) P. B. Karadakov, *Org. Lett.* **2020**, *22*, 8676–8680.

[13] https://github.com/mathnet/mathnet-numerics.

[14] D. Inniss, S. M. Soltis, C. E. Strouse, *J. Am. Chem. Soc.* **1988**, *110*, 5644–5650.

[15] Y. Iimura, T. Sakurai, K. Yamamoto, *Bull. Chem. Soc. Jpn.* **1988**, *61*, 821–822.

[16] W. Jentzen, I. Turowska-Tyrk, W. R. Scheidt, J. A. Shelnutt, *Inorg. Chem.* **1996**, *35*, 3559–3567.

[17] D. L. Cullen, E. F. Meyer, *J. Am. Chem. Soc.* **1974**, *96*, 2095–2102.

[18] T. D. Brennan, W. R. Scheidt, J. A. Shelnutt, *J. Am. Chem. Soc.* **1988**, *110*, 3919–3924.

[19] E. F. Meyer, *Acta Crystallogr. Sect. B* **1972**, *28*, 2162–2167.

[20] L. J. Pace, A. Ulman, J. A. Ibers, *Inorg. Chem.* **1982**, *21*, 199–207.

[21] K. M. Barkigia, M. W. Renner, L. R. Furenlid, C. J. Medforth, K. M. Smith, J. Fajer, *J. Am. Chem. Soc.* **1993**, *115*, 3627–3635.

[22] X.-Z. Song, W. Jentzen, S.-L. Jia, L. Jaquinod, D. J. Nurco, C. J. Medforth, K. M. Smith, J. A. Shelnutt, *J. Am. Chem. Soc.* **1996**, *118*, 12975–12988.

[23] M. O. Senge, C. J. Medforth, T. P. Forsyth, D. A. Lee, M. M. Olmstead, W. Jentzen, R. K. Pandey, J. A. Shelnutt, K. M. Smith, *Inorg. Chem.* **1997**, *36*, 1149–1163.

[24] E. B. Fleischer, C. K. Miller, L. E. Webb, *J. Am. Chem. Soc.* **1964**, *86*, 2342–2347.

[25] T. Nagata, A. Osuka, K. Maruyama, K. Toriumi, *Acta Crystallogr. Sect. C* **1990**, *46*, 1745–1747.

[26] M. Mazzanti, J.-C. Marchon, M. Shang, W. R. Scheidt, S. Jia, J. A. Shelnutt, *J. Am. Chem. Soc.* **1997**, *119*, 12400–12401.

[27] M. O. Senge, K. Ruhlandt-Senge, K. J. Regli, K. M. Smith, *J. Chem. Soc. Dalton Trans.* **1993**, 3519–3538.

[28] B. M. Chen, A. Tulinsky, *J. Am. Chem. Soc.* **1972**, *94*, 4144–4151.

[29] J. W. Lauher, J. A. Ibers, *J. Am. Chem. Soc.* **1973**, *95*, 5148–5152.

[30] D. J. Nurco, C. J. Medforth, T. P. Forsyth, M. M. Olmstead, K. M. Smith, *J. Am. Chem. Soc.* **1996**, *118*, 10918–10919.

[31] a) M. Bröring, F. Brégier, E. Cónsul Tejero, C. Hell, M. C. Holthausen, *Angew. Chem. Int. Ed.* **2007**, *46*, 445–448; *Angew. Chem.* **2007**, *119*, 449–452; b) K. E. Thomas, J. Conradie, L. K. Hansen, A. Ghosh, *Inorg. Chem.*

2011, *50*, 3247–3251; c) K. E. Thomas, A. B. Alemayehu, J. Conradie, C. M. Beavers, A. Ghosh, *Acc. Chem. Res.* **2012**, *45*, 1203–1214.
[32] J.-i. Setsune, *Chem. Rev.* **2017**, *117*, 3044–3101.
[33] a) A. Ghosh, K. Jynge, *Chem. Eur. J.* **1997**, *3*, 823–833; b) T. Ding, J. D. Harvey, C. J. Ziegler, *J. Porphyrins Phthalocyanines* **2005**, *9*, 22–27.
[34] M. Bröring, M. Cordes, S. Köhler, *Z. Anorg. Allg. Chem.* **2008**, *634*, 125–130.
[35] https://github.com/JensKrumsieck/ChemSharp.
[36] https://github.com/oxyplot/oxyplot.
[37] https://github.com/helix-toolkit/helix-toolkit.
[38] https://github.com/MaterialDesignInXAML/MaterialDesignInXamlToolkit, http://github.com/JensKrumsieck/TinyMVVM, http://github.com/JensKrumsieck/ThemeCommons.

Manuscript received: April 7, 2021
Accepted manuscript online: June 1, 2021
Version of record online: June 24, 2021

